


Kohn-Sham Theory of the Fractional Quantum Hall Effect

Yayun Hu  and J. K. Jain 

Physics Department, Pennsylvania State University, 104 Davey Laboratory, University Park, Pennsylvania 16802, USA

 (Received 15 July 2019; published 25 October 2019)

We formulate the Kohn-Sham (KS) equations for the fractional quantum Hall effect by mapping the original electron problem into an auxiliary problem of composite fermions that experience a density dependent effective magnetic field. Self-consistent solutions of the KS equations demonstrate that our formulation captures not only configurations with nonuniform densities but also topological properties such as fractional charge and fractional braid statistics for the quasiparticles excitations. This method should enable a realistic modeling of the edge structure, the effect of disorder, spin physics, screening, and of fractional quantum Hall effect in mesoscopic devices.

DOI: [10.1103/PhysRevLett.123.176802](https://doi.org/10.1103/PhysRevLett.123.176802)

The Kohn-Sham density functional theory (KS-DFT) uses the electron density to construct a single particle formalism that incorporates the complex effects of many-particle interactions through a universal exchange correlation functional [1]. It is an invaluable tool for treating systems of interacting electrons spanning the disciplines of physics, chemistry, materials science, and biology. Very little work has been done [2–4] toward applying this method to the fractional quantum Hall effect (FQHE) [5], which is one of the most remarkable manifestations of interelectron interactions [6,7]. The reasons are evident. To begin with, even though the KS-DFT is in principle exact, its accuracy, in practice, is dictated by the availability of exchange correlation (xc) potentials, and it works best when the xc contribution is small compared to the kinetic energy. In the FQHE problem, the kinetic energy is altogether absent (at least in the convenient limit of very high magnetic fields) and the physics is governed entirely by the xc energy. A more fundamental impediment is that, by construction, the KS-DFT eventually obtains a single Slater determinant solution, whereas the ground state for the FQHE problem is an extremely complex, filling factor-dependent wave function that is not adiabatically connected to a single Slater determinant. In particular, a mapping into a problem of noninteracting electrons in a KS potential will produce a ground state that locally has integer fillings, whereas nature displays preference for certain fractional fillings. Finally, a mapping into a system of weakly interacting electrons will also fail to capture topological features of the FQHE, such as fractional charge and fractional braid statistics for the quasiparticles [6,8,9]. At a fundamental level, these difficulties can be traced back to the fact that the space of ground states in the lowest Landau level (LLL) is highly degenerate for noninteracting electrons, and the interaction causes a nonperturbative reorganization to produce the FQHE. We note here that the application of KS-DFT to “strictly correlated electrons” is

in general an important problem and has previously been considered in other contexts [10–13].

To make progress, we exploit the fact that the strongly interacting electrons in the FQHE regime turn into weakly interacting composite fermions, namely bound states of electrons and an even number ($2p$) of quantum vortices [7,14]. This suggests using an auxiliary system of noninteracting composite fermions to construct a KS-DFT formulation of the FQHE, which is the approach we follow in this work. A crucial aspect of our KS theory is that it properly incorporates the physics of the long range “gauge interaction” between composite fermions induced by the Berry phases due to the quantum mechanical vortices attached to them, which is responsible for the topological properties of the FQHE, such as fractional charge and statistics [7,15,16]. That effectively amounts to using a nonlocal exchange-correlation potential. Earlier DFT formulations of the FQHE [2–4] employ a local exchange-correlation potential and thus do not capture the topological features of the FQHE.

We consider the Hamiltonian for fully spin polarized electrons confined to the LLL:

$$\mathcal{H} = \hat{H}_{ee} + \int d\mathbf{r} V_{\text{ext}}(\mathbf{r}) \hat{\rho}(\mathbf{r}). \quad (1)$$

Within the so-called magnetic-field DFT [17–20], the Hohenberg-Kohn (HK) theorem also applies to interacting electrons in the FQHE regime and implies that the ground state density and energy can be obtained by minimizing the energy functional

$$E[\rho] = F[\rho] + \int d\mathbf{r} V_{\text{ext}}(\mathbf{r}) \rho(\mathbf{r}), \quad (2)$$

where the HK functional is given by [21,22]

$$F[\rho] = \min_{\Psi_{\text{LLL}} \rightarrow \rho(\mathbf{r})} \langle \Psi_{\text{LLL}} | \hat{H}_{\text{ec}} | \Psi_{\text{LLL}} \rangle \equiv E_{\text{xc}}[\rho] + E_H[\rho]. \quad (3)$$

(The B dependence of the energy functional has been suppressed for notational convenience). Here $E_{\text{xc}}[\rho]$ and $E_H[\rho]$ are the xc and Hartree energy functionals of electrons and Ψ_{LLL} represents a LLL wave function. The conventional KS mapping into noninteracting electrons is problematic due to the absence of kinetic energy.

We instead map the FQHE into the auxiliary problem of “noninteracting” composite fermions. Composite fermions’ most fundamental property is that they experience an effective magnetic field. In particular, the integer quantum Hall effect of composite fermions at $\nu^* = n$ manifests as the FQHE of electrons at $\nu = n/(2pn \pm 1)$. (The quantities referring to composite fermions are marked by an asterisk below.) Even though we use the term noninteracting, the Berry phases associated with the bound vortices induce a long range gauge interaction between composite fermions, as a result of which they experience a density dependent magnetic field $B^*(\mathbf{r}) = B - 2\rho(\mathbf{r})\phi_0$, where $\phi_0 = hc/e$ is a flux quantum. We therefore write

$$\left[\frac{1}{2m^*} \left(\mathbf{p} + \frac{e}{c} \mathbf{A}^*(\mathbf{r}; [\rho]) \right)^2 + V_{\text{KS}}^*(\mathbf{r}) \right] \psi_\alpha(\mathbf{r}) = \epsilon_\alpha \psi_\alpha(\mathbf{r}), \quad (4)$$

where $V_{\text{KS}}^*(\mathbf{r})$ is the KS potential for composite fermions, m^* is the composite-fermion (CF) mass, and $\nabla \times \mathbf{A}^*(\mathbf{r}; [\rho]) = B^*(\mathbf{r})$. As a result of the gauge interaction, the solution for any given orbital depends, through the $\rho(\mathbf{r})$ dependence of the vector potential, on the occupation of all other orbitals. Equation (4) must therefore be solved self-consistently; i.e., the single-CF orbitals $\psi_\alpha(\mathbf{r})$ must satisfy the condition that the ground state density $\rho(\mathbf{r}) = \sum_\alpha c_\alpha |\psi_\alpha(\mathbf{r})|^2$, where $c_\alpha = 1$ (0) for the lowest energy occupied (higher energy unoccupied) single-CF orbitals, is equal to the density that appears in the kinetic energy of the Hamiltonian. The energy levels of Eq. (4) are Landau-like levels of composite fermions, called Λ levels (Λ LS). For the special case of a spatially uniform density and constant V_{KS}^* , Eq. (4) reduces to the problem of noninteracting particles in a uniform B^* . Importantly, once a self-consistent solution is found for a given $V_{\text{KS}}^*(\mathbf{r})$, for the corresponding density in the Hamiltonian in Eq. (4), the ground state satisfies, by definition, the self-consistency condition and also the variational theorem, and the standard proof for the HK theorem follows. See Supplementary Material [23] for details. We define the CF kinetic energy functional as

$$T_s^*[\rho] = \min_{\Psi \rightarrow \rho} \langle \Psi | \frac{1}{2m^*} \sum_{j=1}^N \left[\mathbf{p}_j + \frac{e}{c} \mathbf{A}^*(\mathbf{r}_j; [\rho]) \right]^2 | \Psi \rangle, \quad (5)$$

where we perform a constrained search over all single Slater determinant wave functions Ψ that correspond to the

density $\rho(\mathbf{r})$, following the strategy of the generalized KS scheme [23,24].

The next key step is to write $E_{\text{xc}}[\rho] = T_s^*[\rho] + E_{\text{xc}}^*[\rho]$, or $F[\rho] = T_s^*[\rho] + E_H[\rho] + E_{\text{xc}}^*[\rho]$. (Note that $T_s^*[\rho]$ and thus $E_{\text{xc}}[\rho]$ is a nonlocal functional of the density.) Such a partitioning of $F[\rho]$ can, in principle, always be made given our assumptions but is practically useful only if the $T_s^*[\rho]$ and $E_H[\rho]$ capture the significant part of $F[\rho]$, and the remainder $E_{\text{xc}}^*[\rho]$, called the exchange-correlation energy of composite fermions, makes a relatively small contribution. This appears plausible given that the CF kinetic energy term captures the topological aspects of the FQHE, and also because the model of weakly interacting composite fermions has been known to be rather successful in describing a large class of experiments.

Minimization of the energy $E[\rho] = T_s^*[\rho] + E_H[\rho] + E_{\text{xc}}^*[\rho] + \int d\mathbf{r} V_{\text{ext}}(\mathbf{r})\rho(\mathbf{r})$ with respect to $\rho(\mathbf{r}) = \sum_\alpha c_\alpha |\psi_\alpha(\mathbf{r})|^2$, subject to the constraint $\int d\mathbf{r} \psi_\alpha^*(\mathbf{r})\psi_\beta(\mathbf{r}) = \delta_{\alpha\beta}$, yields [23] Eq. (4) with

$$V_{\text{KS}}^*[\rho, \{\psi_\alpha\}] = V_H(\mathbf{r}) + V_{\text{xc}}^*(\mathbf{r}) + V_{\text{ext}}(\mathbf{r}) + V_T^*(\mathbf{r}), \quad (6)$$

where $V_H(\mathbf{r}) = \delta E_H / \delta \rho(\mathbf{r})$ and $V_{\text{xc}}^*(\mathbf{r}) = \delta E_{\text{xc}}^* / \delta \rho(\mathbf{r})$ are the Hartree and CF-xc potentials. The nonstandard potential

$$V_T^*(\mathbf{r}) = \sum_\alpha c_\alpha \langle \psi_\alpha | \frac{\delta T_s^*}{\delta \rho(\mathbf{r})} | \psi_\alpha \rangle \quad (7)$$

with $T_s^* = (1/2m^*)[\mathbf{p} + (e/c)\mathbf{A}^*(\mathbf{r}; [\rho])]^2$ arises due to the density dependence of the CF kinetic energy. V_T^* describes the change in T_s^* to a local disturbance in density for a fixed choice of the KS orbitals. Equations (4)–(7) define our KS equations. Because $V_T^*(\mathbf{r})$ depends not only on the density but also on the occupied orbitals, we are actually working with what is known as the “orbital dependent DFT” [25].

Having formulated the CF-DFT equations, we now proceed to obtain solutions for some representative cases. The primary advantage of our approach is evident without any calculations. Take the example of a uniform density FQHE state at $\nu = n/(2pn \pm 1)$. It is an enormously complicated state in terms of electrons but maps into the CF state at filling factor $\nu^* = n$ with a spatially uniform magnetic field, thereby producing the correct density without any fine-tuning of parameters or averaging. For nonuniform densities, the state of noninteracting composite fermions will produce configurations where composite fermions *locally* have $\nu^* \approx n$, which corresponds to an electronic state where the local filling factor is $\nu \approx n/(2pn \pm 1)$, which is a reasonable description, and certainly a far superior representation of the reality than any state of noninteracting electrons.

For a more quantitative treatment we need a model for the xc energy. To this end, we begin by making the local density approximation (LDA) to write $E_{\text{xc}}^*[\rho] = \int d\mathbf{r} \epsilon_{\text{xc}}^*[\rho(\mathbf{r})]\rho(\mathbf{r})$,

where $\epsilon_{xc}^*[\rho]$ is the xc energy per CF. In the following, we express all lengths in units of the magnetic length $l_B = \sqrt{\hbar c/eB}$ and energies in units of e^2/el_B , where ϵ is the dielectric constant of the background. The density is related to the local filling factor as $\nu(\mathbf{r}) = \rho(\mathbf{r})2\pi l_B^2$. We take the model $\epsilon_{xc}^*[\rho] = a\nu^{1/2} + (b-f/2)\nu + g$, with $a = -0.78213$, $b = 0.2774$, $f = 0.33$, $g = -0.04981$. The form is chosen so that the sum of ϵ_{xc}^* and CF kinetic energy accurately reproduces the known electronic xc energies at $\nu = n/(2n+1)$ [23]. (The term $a\nu^{1/2}$ is chosen to match with the known classical value of energy of the Wigner crystal in the limit $\nu \rightarrow 0$ [26].) Although optimized for $\nu = n/(2n+1)$, we will uncritically assume this form of $\epsilon_{xc}^*(\nu)$ for all ν . Our aim in this work is to establish the proof-of-principle validity and the applicability of our approach and its ability to capture topological features; a more extensive search for the most optimal E_{xc}^* is left for future work. The topological properties we focus on in this Letter are largely robust against the precise form of the xc energy. The xc potential is given by $V_{xc}^* = \delta E_{xc}^*/\delta\rho(\mathbf{r}) = \frac{3}{2}a\nu^{1/2} + (2b-f)\nu + g$. We note that while the CF xc potential V_{xc}^* is a continuous function of density, the *electron* xc potential V_{xc} has derivative discontinuities at $\nu = n/(2n \pm 1)$, arising from the kinetic energy of the composite fermions [23].

In our applications below, we will consider N electrons in a potential $V_{\text{ext}}(\mathbf{r}) = -\int d^2\mathbf{r}' \frac{\rho_b(\mathbf{r}')}{\sqrt{|\mathbf{r}-\mathbf{r}'|^2+d^2}}$ generated by a two-dimensional uniform background charge density $\rho_b = \nu_0/2\pi l_B^2$ distributed on a disk of radius R_b , satisfying $\pi R_b^2 \rho_b = N$ at a separation of d from the plane of the electron liquid. This produces an electron system at filling factor $\nu = \nu_0$ in the interior of the disk. We use $\nu_0 = 1/3$ and $d/l_B \rightarrow 0$ in our calculations below. For the vector potential, we assume circular symmetry and choose the gauge $\mathbf{A}^*(\mathbf{r}) = [r\mathcal{B}(r)/2]\mathbf{e}_\phi$, with $\mathcal{B}(r) = (1/\pi r^2) \int_0^r 2\pi r' B^*(r') dr'$.

We obtain self-consistent solutions of Eqs. (4)–(7) by an iterative process. Even though we are interested in the zero temperature limit in this Letter, we sometimes find it useful to begin with a finite temperature $k_B T \sim 0.1$, and anneal the system to approach successively lower temperatures [23,27].

As a first application, we consider the density profile of the $\nu_0 = 1/3$ droplet. Figure 1 shows the density profiles calculated from Laughlin's trial wave function [6] as well as that obtained from exact diagonalization at total angular momentum $L = 3N(N-1)/2$ [28]. Also shown are the density profiles obtained from the above KS equations. The density profile from our CF-DFT captures that obtained in exact diagonalization well, especially for $N \geq 10$. Remarkably, it reproduces the characteristic shape near the edge where the density exhibits oscillations and overshoots the bulk value before descending to zero. This qualitative behavior is fairly insensitive to the choice of

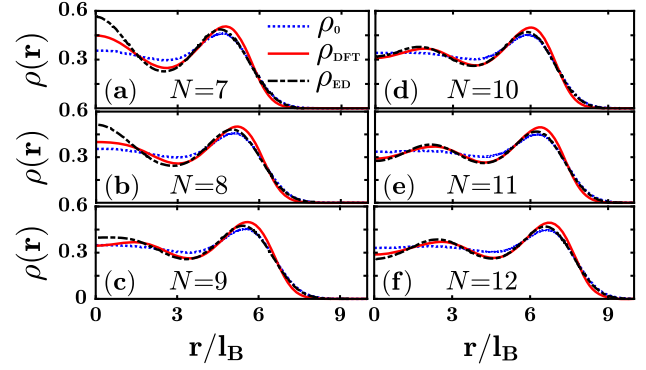


FIG. 1. Density profile for $1/3$ droplets. This figure shows the density of a system of N composite fermions. ρ_0 is the density for Laughlin's $1/3$ wave function [6], and ρ_{ED} is obtained from exact diagonalization (ED) of the Coulomb interaction at total angular momentum $L_{\text{total}} = 3N(N-1)/2$ [28]. The density ρ_{DFT} is calculated from the solution of the KS equations for composite fermions in an external potential produced by a uniform positively charged disk of radius R so that $\pi R^2 \rho_b = N$. The total angular momentum of the CF state is L_{tot}^* , which is related to the total angular momentum of the electron state by $L_{\text{tot}} = L_{\text{tot}}^* + N(N-1)$ [29]. The CF-DFT solution produces $L_{\text{tot}}^* = N(N-1)/2$, which is consistent with $L_{\text{tot}} = 3N(N-1)/2$. All densities are quoted in units of $(2\pi l_B^2)^{-1}$, the density at $\nu = 1$. We take $\rho_b = 1/3$.

V_{xc}^* , and is largely a result of the self-consistency requirement in Eq. (4) [23]. The Supplemental Material [23] considers other configurations, and also shows that a mean-field approximation without self-consistency is highly unsatisfactory for the density profile.

We next consider screening of an impurity with charge $Q = \pm e$ at a height h directly above the center of the FQHE droplet. The strength of its potential

$$V_{\text{imp}}(\mathbf{r}) = \frac{Q}{\sqrt{|\mathbf{r}|^2 + h^2}} \quad (8)$$

can be tuned by varying h . Figures 2(a) through 2(e) show the density ρ for certain representative values of h . It is important to note that the CF orbitals in the self-consistent solution form strongly renormalized Λ s (i.e., include the effect of mixing between the unperturbed Λ s). Figures 2(f) through 2(j) show the occupation of the Λ s. The presence of the impurity either empties some CF orbitals from the lowest Λ or fills those in higher Λ s. Each empty orbital in the lowest Λ corresponds to a charge $1/3$ quasihole, whereas each filled orbital in an excited Λ corresponds to a charge $-1/3$ quasiparticle [7]. The excess charge is defined as $\delta q = \int_{|\mathbf{r}| < r_0} d^2\mathbf{r} [\rho_0 - \rho(\mathbf{r})]$ in a circular area of radius $r_0 = 10l_B$ around the origin. Figure 2(p) shows how δq and L_{tot}^* change as a function of the impurity potential at the origin $V_{\text{imp}}(\mathbf{r} = 0) = -Q/h$.

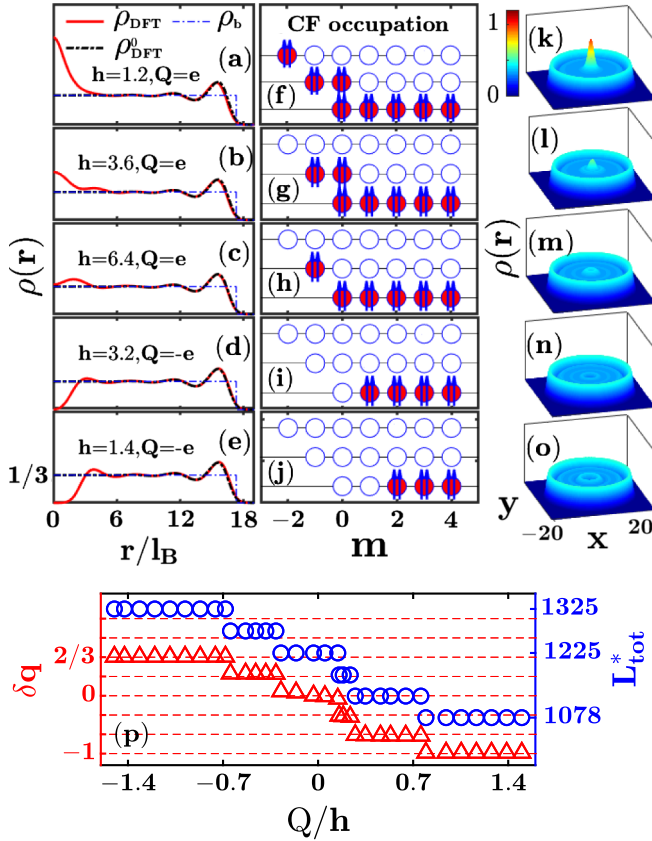


FIG. 2. Screening and fractional charge. This figure shows how the $1/3$ state screens a charged impurity of strength $Q = \pm e$ located at a perpendicular distance h from the origin. (a)–(e), (k)–(o) Self-consistent density $\rho_{\text{DFT}}(\mathbf{r})$. Also shown are $\rho_{\text{DFT}}^0(\mathbf{r})$, the “unperturbed” density (for $Q = 0$), and ρ_b , which is the density of the positively charged background. (f)–(j) Occupation of renormalized Λ Ls in the vicinity of the origin; each composite fermion is depicted as an electron with two arrows, which represent quantized vortices. (The single particle angular momentum is given by $m = -n, -n + 1, \dots$ in the n th Λ L.) (p) Evolution of the excess charge δq and the total CF angular momentum L_{tot}^* as a function of the impurity potential strength at the origin $V_{\text{imp}}(r = 0) = Q/h$. Change in the charge at the origin is associated with a change in L_{tot}^* . The system contains a total of $N = 50$ composite fermions. For $h = \infty$, we have $L_{\text{tot}}^* = 1225$ and $\delta q = 0$. For one and two quasipoles, we have $L_{\text{tot}}^* = 1225$ and 1275 , whereas for one, two, and three quasiparticles we have $L_{\text{tot}}^* = 1175, 1127$, and 1078 , precisely as expected from the configurations in (f)–(j) [29].

The excess charge δq is seen to be quantized at an integer multiple of $\pm 1/3$.

We finally come to fractional braid statistics. Particles obeying such statistics, called anyons, are characterized by the property that the phase associated with a closed loop of a particle depends on whether the loop encloses other particles. In particular, for Abelian anyons, each enclosed particle contributes a phase factor of $e^{i2\pi\alpha}$, where α is called the statistics parameter. [For noninteracting bosons

(fermions), α is an even (odd) integer.] In the FQHE, the quasiparticles are excited composite fermions and quasiholes are “missing” composite fermions. Let us consider quasiholes of the $1/3$ state for illustration. A convenient way to ascertain the statistics parameter within our KS-DFT is to ask how the location of a quasihole in angular momentum m orbital changes when another quasihole is inserted at the origin in the $m = 0$ orbital. Let us first recall what is the expected behavior arising from fractional braid statistics. In an effective description, the wave function of a single quasihole in angular momentum m orbital is given by $z^m e^{-|z|^2/4l_B^2}$ ($z \equiv x - iy$), which is maximally localized at $r_{\text{ex}} = (2m)^{1/2}l_B^* = (6m)^{1/2}l_B$, with $l_B^* = \sqrt{3}l_B$ (as appropriate for $\nu_0 = 1/3$). When another quasihole is present at the origin, it induces an additional statistical phase factor $e^{i2\pi\alpha}$, where α is the statistics parameter. This changes the wave function of the outer quasihole to $z^{m-\alpha} e^{-|z|^2/4l_B^2}$, which is now localized at $r'_{\text{ex}} = [6(m - \alpha)]^{1/2}l_B$. We now determine α from our KS-DFT formalism.

A quasihole can be treated in a constrained DFT [30] wherein we leave a certain angular momentum orbital unoccupied. Figures 3(a) and 3(b) show the self-consistent KS density profiles of the state with a quasihole in angular momentum m , without and with another quasihole in the $m = 0$ orbital. The locations of the outer quasihole, r_{DFT} and r'_{DFT} , are determined from the minimum in the density. These are in reasonable agreement with the expected positions r_{ex} and r'_{ex} (provided $m > 3$). More importantly, the calculated statistics parameter $\alpha \equiv (r_{\text{DFT}}^2 - r'_{\text{DFT}}^2)/6l_B^2$ is in excellent agreement with the expected fractional value of $\alpha = 2/3$ [7,8] provided that the two quasiparticles are not

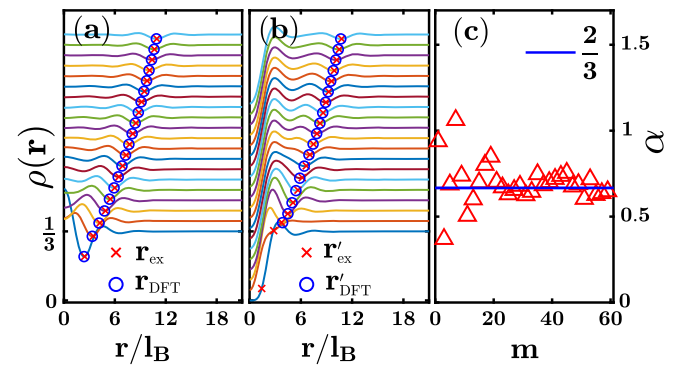


FIG. 3. Fractional braid statistics. (a) Electron density for a system with a quasihole in angular momentum m orbital, with m changing from 1 to 20 for the curves from the bottom to the top. (Each successive curve has been shifted up vertically for clarity.) (b) The same in the presence of another quasihole at the origin. For each m , we indicate the expected position of the outer quasihole (red cross) as well as the position obtained from the DFT density determined by locating the local minimum (blue circle). (c) Calculated statistics parameter $\alpha \equiv (r_{\text{DFT}}^2 - r'_{\text{DFT}}^2)/6l_B^2$. The calculation has been performed for $N = 200$ composite fermions at $\nu_0 = 1/3$.

close to one another, indicating that our method properly captures the physics of fractional braid statistics. The small deviation from $2/3$ for large m arises from the fact that the density of the unperturbed system itself has slight oscillations due to the finite system size, which causes a slight shift in the position of the local minimum due to an additional quasihole. Correcting for that effect produces a value much closer to $\alpha = 2/3$, as illustrated in the Supplemental Material [23].

In conclusion, we have formulated in this Letter a Kohn-Sham DFT that faithfully captures the topological characteristics of the FQHE state, such as fractional charge, fractional statistics, and effective magnetic field. This opens a new strategy for exploring a variety of problems of interest. Aside from the nature of FQHE edges, our approach should allow a quantitative treatment of the effect of smooth disorder, as well as of correction due to Landau level mixing and finite width through appropriate modifications of the xc potential. One can anticipate a generalization of the KS-DFT to paired CF states supporting non-Abelian excitations. Modeling of mesoscopic devices should provide important insight into the optimal conditions for the measurement of fractional statistics through interference experiments (e.g., Ref. [31]).

We are grateful to Gerald Knizia, Andre Laestadius, Paul Lammert, Melvyn Levy, and Erik Tellgren for very useful discussions and advice. We acknowledge financial support from the U.S. Department of Energy under Grant No. DE-SC0005042. Y.H. thanks Yang Ge, Jiabin Yu and PSU DFT Cafe for illuminating help, and acknowledges partial financial support from China Scholarship Council. Some of the numerical calculations were performed using the DiagHam package, for which we are grateful to its authors. The numerical calculations were performed using Advanced CyberInfrastructure computational resources provided by the Institute for CyberScience at the Pennsylvania State University. We thank the Indian Institute Science, Bangalore, where part of this work was performed, for their hospitality, and the Infosys Foundation for making the visit possible.

-
- [1] G. Giuliani and G. Vignale, *Quantum Theory of the Electron Liquid* (Cambridge University Press, Cambridge, England, 2008).
- [2] M. Ferconi, M. R. Geller, and G. Vignale, *Phys. Rev. B* **52**, 16357 (1995).
- [3] O. Heinonen, M. I. Lubin, and M. D. Johnson, *Phys. Rev. Lett.* **75**, 4110 (1995).

- [4] J. Zhao, M. Thakurathi, M. Jain, D. Sen, and J. K. Jain, *Phys. Rev. Lett.* **118**, 196802 (2017).
- [5] D. C. Tsui, H. L. Stormer, and A. C. Gossard, *Phys. Rev. Lett.* **48**, 1559 (1982).
- [6] R. B. Laughlin, *Phys. Rev. Lett.* **50**, 1395 (1983).
- [7] J. K. Jain, *Composite Fermions* (Cambridge University Press, New York, 2007).
- [8] B. I. Halperin, *Phys. Rev. Lett.* **52**, 1583 (1984).
- [9] D. Arovas, J. R. Schrieffer, and F. Wilczek, *Phys. Rev. Lett.* **53**, 722 (1984).
- [10] M. Seidl, *Phys. Rev. A* **60**, 4387 (1999).
- [11] M. Seidl, J. P. Perdew, and M. Levy, *Phys. Rev. A* **59**, 51 (1999).
- [12] P. Gori-Giorgi, M. Seidl, and G. Vignale, *Phys. Rev. Lett.* **103**, 166402 (2009).
- [13] F. Malet and P. Gori-Giorgi, *Phys. Rev. Lett.* **109**, 246402 (2012).
- [14] J. K. Jain, *Phys. Rev. Lett.* **63**, 199 (1989).
- [15] G. S. Jeon, K. L. Graham, and J. K. Jain, *Phys. Rev. B* **70**, 125316 (2004).
- [16] Y. Zhang, G. J. Sreejith, N. D. Gemelke, and J. K. Jain, *Phys. Rev. Lett.* **113**, 160404 (2014).
- [17] C. J. Grayce and R. A. Harris, *Phys. Rev. A* **50**, 3089 (1994).
- [18] W. Kohn, A. Savin, and C. A. Ullrich, *Int. J. Quantum Chem.* **100**, 20 (2004).
- [19] E. I. Tellgren, S. Kvaal, E. Sagvolden, U. Ekström, A. M. Teale, and T. Helgaker, *Phys. Rev. A* **86**, 062506 (2012).
- [20] E. I. Tellgren, A. Laestadius, T. Helgaker, S. Kvaal, and A. M. Teale, *J. Chem. Phys.* **148**, 024101 (2018).
- [21] M. Levy, *Proc. Natl. Acad. Sci. U.S.A.* **76**, 6062 (1979).
- [22] E. H. Lieb, *Int. J. Quantum Chem.* **24**, 243 (1983).
- [23] See Supplemental Material at <http://link.aps.org/supplemental/10.1103/PhysRevLett.123.176802> which includes background information, a proof of the Hohenberg-Kohn theorem for noninteracting composite fermions, a generalization to finite temperatures, details of how the KS equation is numerically solved, and a discussion of the importance of self-consistency.
- [24] A. Seidl, A. Görling, P. Vogl, J. A. Majewski, and M. Levy, *Phys. Rev. B* **53**, 3764 (1996).
- [25] S. Kümmel and L. Kronik, *Rev. Mod. Phys.* **80**, 3 (2008).
- [26] L. Bonsall and A. A. Maradudin, *Phys. Rev. B* **15**, 1959 (1977).
- [27] A. Pribram-Jones, S. Pittalis, E. Gross, and K. Burke, in *Frontiers and Challenges in Warm Dense Matter* (Springer, New York, 2014), pp. 25–60.
- [28] E. V. Tsiper and V. J. Goldman, *Phys. Rev. B* **64**, 165311 (2001).
- [29] J. K. Jain and T. Kawamura, *Europhys. Lett.* **29**, 321 (1995).
- [30] B. Kaduk, T. Kowalczyk, and T. Van Voorhis, *Chem. Rev.* **112**, 321 (2012).
- [31] J. Nakamura, S. Fallahi, H. Sahasrabudhe, R. Rahman, S. Liang, G. C. Gardner, and M. J. Manfra, *Nat. Phys.* **15**, 563 (2019).